

SPECTRUM OF TEV GAMMA RAYS FROM THE CRAB NEBULA

D.A.Carter-Lewis¹, S.Biller², P.J.Boyle³, J.H.Buckley⁴, A.Burdett², J.Bussons Gordo³,
M.A.Catanese¹, M.F.Cawley⁵, D.J.Fegan³, J.P.Finley⁶, J.A.Gaidos⁶,
A.M.Hillas², F.Krennrich¹, R.C.Lamb⁷, R.W.Lessard⁶, C.Masterson³, J.E.McEnery³,
G.Mohanty¹, J.Quinn³, A.J.Rodgers², H.J.Rose², F.W.Samuelson¹, G.H.Sembroski⁶,
R.Srinivasan⁶, T.C.Weekes⁴, M.West,² J.A.Zweerink¹

¹ *Iowa State University, U.S.A.*

² *University of Leeds, United Kingdom.*

³ *University College, Dublin, Ireland*

⁴ *Whipple Observatory, Harvard-Smithsonian CfA, U.S.A.*

⁵ *St.Patrick's College, Maynooth, Ireland*

⁶ *Purdue University, U.S.A.*

⁷ *Space Radiation Lab, Caltech, U.S.A.*

ABSTRACT

The Crab Nebula has become established as the standard candle for TeV gamma-ray astronomy using the atmospheric Cherenkov technique. No evidence for variability has been seen. The spectrum of gamma rays from the Crab Nebula has been measured in the energy range 500 GeV to 8 TeV at the Whipple Observatory by the atmospheric Cherenkov imaging technique. Two methods of analysis involving independent Monte Carlo simulations and two databases of observations (1988-89 and 1995-96) were used and gave close agreement. Using the complete spectrum of the Crab Nebula, the spectrum of relativistic electrons is deduced and the spectrum of the resulting inverse Compton gamma-ray emission is in good agreement with the measured spectrum if the ambient magnetic field is about 25-30 nT.

1. INTRODUCTION

The Crab Nebula has become a standard candle in TeV astronomy; it has been detected by many groups and its integral flux appears constant. (We refer to the “steady” emission, not emission modulated at the pulsar period. We have not detected the latter at TeV energies. See paper by G. Gillanders et al., in these proceedings.) It is also well on the way to becoming a standard candle with regard to TeV spectral content. Synchrotron emission from the Crab covers a remarkably broad range terminating at about 10^8 eV, where a new component attributed to inverse Compton scattering begins. It is this component that we detect. The TeV spectrum is sensitive to the primary electron spectrum, the nebular magnetic field and the spatial distribution of electrons and magnetic field within the nebula.

In this paper we briefly describe two methods for extracting TeV spectra, compare results from the Whipple Observatory Imaging Cherenkov Telescope for the 1988/89 and 1995/96 observing seasons and comment on implications for the physics of the nebula. The methods, developed at Iowa State University and the University of Leeds, are based on Monte Carlo simulations using completely independent code and use different approaches in determining the overall gain of the Cherenkov telescope. In the ISU approach, the gains of the photomultiplier tubes, mirror reflectivities, etc., are measured and combined to find the overall gain. In the Leeds approach, the observed brightness distribution of cosmic-ray images is combined with cosmic-ray simulation results to determine the overall gain of the telescope. The methods are described in detail in “Paper I,” Mohanty et al., (1997), and the resulting TeV spectrum is put into context of other observations with implications for the physics of the nebula in “Paper II,” Hillas et al., (1997). The latter paper also compares our Crab TeV spectrum with those of other groups.

A straightforward approach to the determination of TeV spectra was developed at Iowa State University. Three components are required. First, a method of distinguishing gamma-ray images from background cosmic-ray images. The standard method is to use “supercuts” as described in, e.g., Punch et al. (1996). The images are characterized by second order moments giving the *width*, *length*, *distance* of the image centroid from the optic axis and *alpha*, the angle by which the image major axis misses passing through the optic axis. More than 99% of the background can be rejected by requiring small values of *width*, *length* and *alpha*. However, this procedure results in a strong bias against the images of higher energy gamma rays which tend to be longer and broader and hence more cosmic-ray like. Mohanty (1995) has modified the procedure so that the image selection criteria depend on the total brightness or *size* of the image as well. (The *size* can be used as an estimate of the energy.) The telescope collection areas for simulated gamma rays for the 1995/96 season using standard and “extended” supercuts is shown in Fig. 1.

The second component needed is a way to estimate the energy of each gamma-ray image. Two desirable criteria are (a) good resolution and (b) negligible bias. The former is important to detect small structures in the spectrum and the latter is important to avoid distortions. We obtained a resolution of $\Delta E/E \sim 0.36$ with negligible bias by using a second order polynomial in *size* and *distance* as described in Paper I. The energy resolution function is, to a good approximation, Gaussian in the variable $\log(E)$. It is plotted at an arbitrary energy in Fig. 1.

In data taken for spectral analysis, each on-source observation is followed by an “off-source” observation covering the same range of range of azimuth and elevation angles. The images for both types of observation are selected for gamma-like events. The estimated energies from corresponding observations are histogrammed and the difference ascribed to gamma rays from the source. This can then be fit by a power law or the fluxes extracted as described in Paper I.

3. METHOD 2: AN INTUITIVE APPROACH

A different approach with emphasis on verifiability was developed at the University of Leeds. There are two pieces to this approach, a method for selecting images likely to have been initiated by cosmic gamma rays and a method for determining the primary gamma-ray energy spectrum from the observed *size* spectra. Earlier descriptions of this approach are in (Hillas and West, 1991) and (West, 1994).

The selection criterion is a “cluster” or “spherical” method in which a single parameter is used to characterize the gamma-ray-like nature of an image and correlations between image parameters are incorporated naturally. Simulated gamma rays produce images with four parameters (*width*, *length*, *distance* and *alpha*) that populate a four-dimensional space. Each real image can be tested to see if it is likely to be a gamma-ray image by the value of the Mahalanobis distance between it and the centroid of the cluster. (This is equivalent to scaling and rotation of the axes so that the window is spherical and fluctuations uncorrelated.) The selection window is defined by the expected position and dimensions of the gamma-ray parameter cluster for several broad ranges of image *size*.

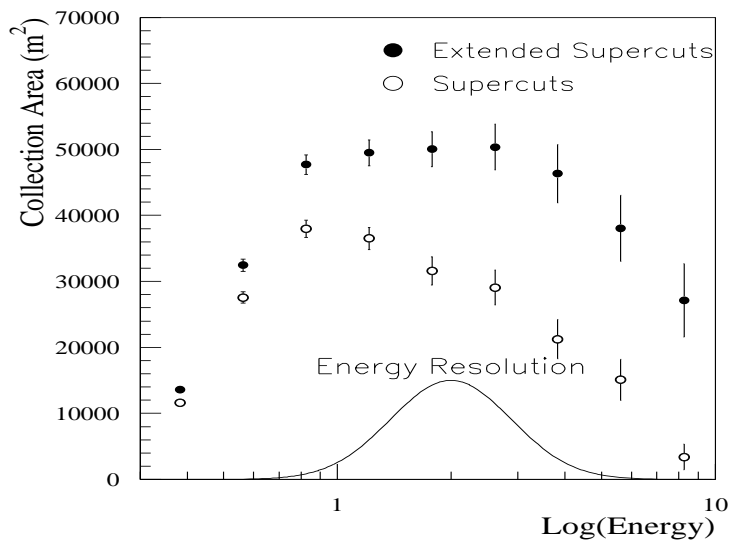


Fig. 1: The collection areas for standard and extended supercuts for the 1995/96 observing season are shown above. The resolution function is also plotted.

observations and the difference histogram is ascribed to gamma rays. A simulated *size* spectrum is then computed starting with a power-law primary energy spectrum for gamma rays. A weight is given to each simulated gamma ray and, by adjusting these weights, the spectrum can be varied so that its *size* spectrum matches that of the difference histogram. This method is simple, easy to implement and avoids the complexity of calculating collection areas and bias-free energy estimates. It is described in detail in Paper I.

4. RESULTS

The spectra obtained from the 1988/89 and 1995/96 seasons using Method 1 and 1988/89 season using Method 2 are in good agreement as shown in Fig. 2. As described in Paper I, we have tested the sensitivity of the results to uncertainties in the Monte Carlo simulations and have found that the results are relatively robust. The combined TeV fluxes from both seasons from Method 1 are well fit with the simple power law spectrum in which the differential flux ($J(E)$) is given by:

$$(3.3 \pm .2 \pm .7) 10^{-7} \left(\frac{E}{\text{TeV}}\right)^{-2.45 \pm .08 \pm .05} \quad (1)$$

in units of $\text{m}^{-2} \text{s}^{-1} \text{TeV}^{-1}$ where the first errors are statistical and the second are our estimate of systematic errors.

However, the simple extrapolation of this fit to lower energies yields fluxes far in excess of those observed by EGRET as is clear from Fig. 3 which shows a quadratic fit of $\log(J)$ vs. $\log(E)$ to our data and to an averaged point representing the EGRET flux (Nolan et al., 1993) at 2 GeV. This fit may be written:

$$J(E) = (3.25) 10^{-7} (E/\text{TeV})^{-2.44-0.135\log_{10}(E)} \text{m}^{-2} \text{s}^{-1} \text{TeV}^{-1}. \quad (2)$$

5. COMMENTS ON INTERPRETATION

Most of the early inverse Compton models for TeV gamma rays assumed a constant magnetic field in the principal source region where these are produced (e.g., Gould 1965 or Rieke and Weekes 1969) whereas more recent models (De Jager and Harding, 1992 or Aharonian and Atoyan) incorporate hydrodynamic plasma/field flow making the calculations more complex and the results probably more realistic. Here, we try to stay close to the data and make the simpler assumption that the field is constant. The broad synchrotron emission band apparently extends up to 10^8 eV and is boosted to higher energies via inverse Compton scattering. The scattering giving rise to TeV gamma rays occurs in the Klein-Nishina rather than in the Thomson scattering regime. This implies that the electrons giving rise to our detected gamma rays must have energies in the range of 2-10 TeV and the corresponding scattered photons would mostly have energies of about 0.005 to 0.3 eV. This conclusion is only very weakly model dependent (see Paper II). Since electrons with energies of a few TeV generate synchrotron radiation at about 0.4 keV in a field of about 25 nT (see next paragraph), the

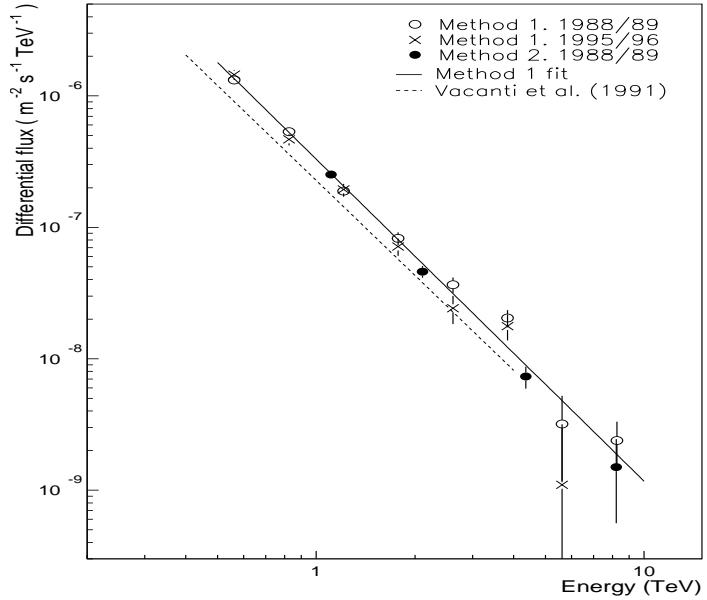


Fig. 2: The Crab spectrum in the range 0.3 to about 8 TeV extracted using Methods 1 (open circles) and 2 (solid circles) for the Whipple 1988/89 database and using Method 1 (x's) for the 1995/96 database are shown above. Also shown is a fit to the combined Method 1 results (solid line) as well as an earlier spectrum (dashed line) taken from Vacanti et al. (1991).

emitting TeV gamma rays.

For assumed magnetic field values and the observed synchrotron flux, it is possible to deduce the spectrum of primary electrons, presumably generated in the shock at the termination of the pulsar wind (see, e.g., Coroniti and Kennel 1985). From the ambient photon density and deduced electron spectrum, the TeV flux can be calculated, and results for B fields of 10, 20 and 40 nT are shown in Fig. 3. The shaded regions reflect uncertainties arising from ill-defined UV to soft-X-ray region of the synchrotron photon spectrum. As can be seen from the figure, the effective B field must lie between 20 and 40 nT with 27 nT falling very near to our TeV data. Since even more energetic electrons only keep their energy for a short time, they should exist only near the pulsar wind shock. Hence, measurement of the TeV spectrum over a wider energy range may probe spatial variations in the nebular magnetic field (see Paper II).

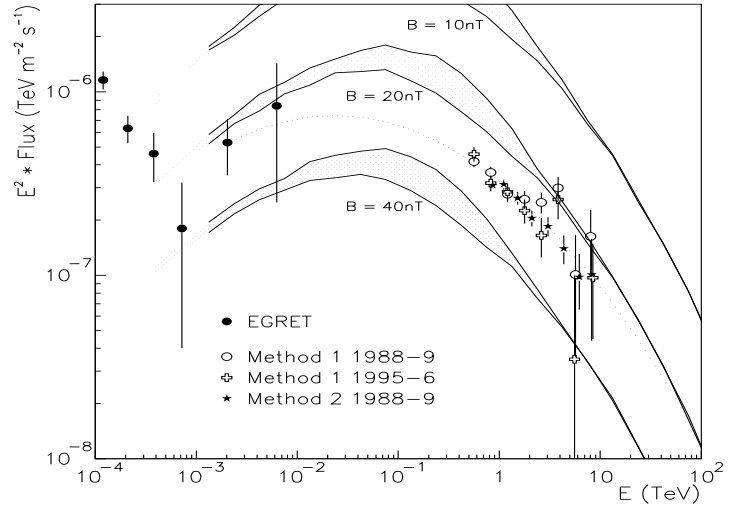


Fig. 3: Whipple and EGRET observations of the Crab gamma-ray spectrum. The dotted line is a fit to the WHipple points and a single 2 GeV flux value. Full-line curves are predicted inverse Compton fluxes for 3 different assumed B fields.

6. ACKNOWLEDGEMENT

This work is supported by grants from the US DOE and NASA, by PPARC in the UK and by Forbairt in Ireland.

7. REFERENCES

- Aharonian, F.A. and Atoyan A.M, *Astropart. Phys.* **3**, 275 (1995)
Atoyan, A.M. and Aharonian, F.A., *MNRAS* **278** 525 (1996).
Coroniti, F.V. and Kennel, C.F., in “The Crab Nebula and related supernova remnants,” ed. M.C.Kafatos and R.B.C. Henry, CUP, p 25 (1985).
De Jager, O.C., and Harding, A.K., *Ap. J.*, **396**, 161 (1992).
Gould, R.J., *Phys. Rev. Lett.*, **15**, 577 (1965).
Harnden, F.R., Jr. and Seward, F.D., *Ap. J.* **283** 279 (1984).
Hillas, A.M. and West, M., *Proc. 22nd ICRC Dublin* **6** 472 (1991).
Hillas, A.M., et al, “Paper II,” to be submitted to *Ap. J.* (1997).
Mohanty, G., PhD Thesis Iowa State University (1995).
Mohanty, G., et al., “Paper I,” *Astroparticle Physics*, submitted (1997).
Nolan, P.L. et al., *Ap. J.*, **409**, 697 (1993).
Punch, M., et al., *Proc. 22nd ICRC Dublin* **1** 464 (1991).
Rieke, G.H., and Weekes, T.C., *Ap. J.*, **155**. 429 (1969).
Vacanti, G., et al., *Ap. J.* **377**, 467 (1991).
West, M., PhD Thesis University of Leeds (1994).